

## A Method for Improving the Positioning Accuracy of Linear Pneumatic Actuators

**Mihai Avram, Victor Constantin, Constantin Nitu, Constantin Bucsan**

*University "Politehnica" of Bucharest, Romania, (e-mail: m\_avram02@yahoo.com, victor.constantin@upb.ro, constantin.nitu@upb.ro, constantin\_bucsan@yahoo.com)*

---

**Abstract:** The paper proposes a novel method for improving the positioning accuracy of a linear pneumatic system, by means of piezoelectric compensation of the error. The mathematical model of the system is proposed and discussed. Also, the model is simulated and a test is used to determine certain parameters of the system. A test stand is built and the experimental results are presented.

**Keywords:** pneumatic, piezoelectric actuator, positioning, error compensation, high accuracy

---

### 1. INTRODUCTION

The pneumatic actuating systems are largely used in industrial applications due to their important advantages, such as: robustness, simplicity, productivity, high reliability, low cost (Naoki et al., 2014). As the pneumatic power is non-polluting these systems are recommended to be used in food industry, pharmaceuticals, chemical industry and dental technique (Shih and Ming-An, 1998).

The large area of applicability of the pneumatic actuating systems required optimizing the performances and reliability of the system components, integrating of smart sensors within their structure and developing of new control algorithms based on nonlinear models. A new concept – pneutronics – appeared following the synergetic joining of three domains: pneumatics, electronics and informatics.

It is well known that a large number of industrial applications require the displacement of loads in the range of 1...10 [kg] and to position them in certain points of the working stroke with an accuracy of  $\pm 0.02 \dots \pm 0.2$  [mm]. This level of accuracy is easily obtained with electric or hydraulic mechatronic actuating systems, but the price of such a system is very high, so they are recommended only when the cost of the application is justified (Brian et al., 2005).

The pneutronic systems may be taken into account only if their positioning accuracy is improved. But the increase of the positioning accuracy and mainly its preservation in time are yet unsolved problems. Moreover, when moving to the target position and while stationary a series of perturbations occur (variations of the actuated load and of the supply pressure, flow losses etc.), which influence the dynamics of the movement and the preservation of the position and which are difficult to control (Dihovicni and Novak, 2008; Hazem and Bashi, 2009).

There are many references regarding the hardware configuration of pneutronic systems and the used control strategies.

So, a system consisting of pneumatic devices having discrete functioning, which positions the actuated load with an

imposed accuracy is achieved by means of a double stroke pneumatic linear motor (Wang et al., 1996). The control of the input/output flow of the active chambers of the motor is performed by four directional valves having discrete functioning and being mounted in parallel. A fuzzy control algorithm is used, where every lot of signals determines a certain speed of the actuated load. A position sensor is used in the loop for real time control of the load positioning. The use of a fuzzy controller in connection with an empirical model was also reported for pneumatic positioning (Yao et al., 2016)

The accurate speed control of the pneumatic mobile assembly can be achieved by using a hydraulic control circuit (Avram et al., 2011). A proportional device within the hydraulic circuit is used to control the speed of the actuated load and a position transducer is used to control the position of the actuated load. The system has high accuracy and a good frequency response, despite it is a pneumatic system. Such systems are also suitable for sliding mode control (Kolsi-Gdoura et al., 2015; Hodgson et al., 2011) or non-time based control schemes (Richiedei, 2012)

Another currently used system incorporates devices controlled by pulse width modulation (Topcu and Yuksel, 2006). These devices are used to accurately control the input and output flow. Use of such devices implies rigorous testing of their characteristics and including the results in the control algorithm of the system.

Most pneutronic positioning systems integrate proportional devices within their structure (Ning and Bone, 2005; Richer and Yildirim, 2000). This method consists of the proportional control of the flow with an electrical input signal, usually a voltage. The control algorithms are simple, the most used being the PID ones. A higher positioning accuracy may be obtained by compensating the error of the pneumatic system using another type of actuation, usually an electric one (Chen, 2012; Bone and Chen, 2012). The resulted system benefits of the advantages of both a pure pneumatic positioning system (long strokes and high working speed) and an electric system (high accuracy and good response time). The positioning

accuracy of such systems depends on the accuracy of the electric positioning (Yung-Tien et al., 2007).

The goal of this paper is to demonstrate that a high accuracy positioning of a load can be obtained with a low cost control. For industrial systems which work in a repetitive mode, such as robotic manipulators, with the same accurate stroke, an iterative learning control can be applied to a pneumatic linear actuator, combined with a piezoelectric actuator for position fine correction.

2. THE PRINCIPLE SET-UP OF THE SYSTEM

Fig. 1, a shows the principle set-up of the pneumatic positioning system. It consists of the following basic devices: the pneumatic linear motor MPL, the devices for pneumatic power control ERC, the air supply, GPA and the electronic control block, BEC. In order to improve the positioning accuracy, a piezoelectric positioning system (SEP) was added (Fig. 1,b), resulting in a mixed actuating system.

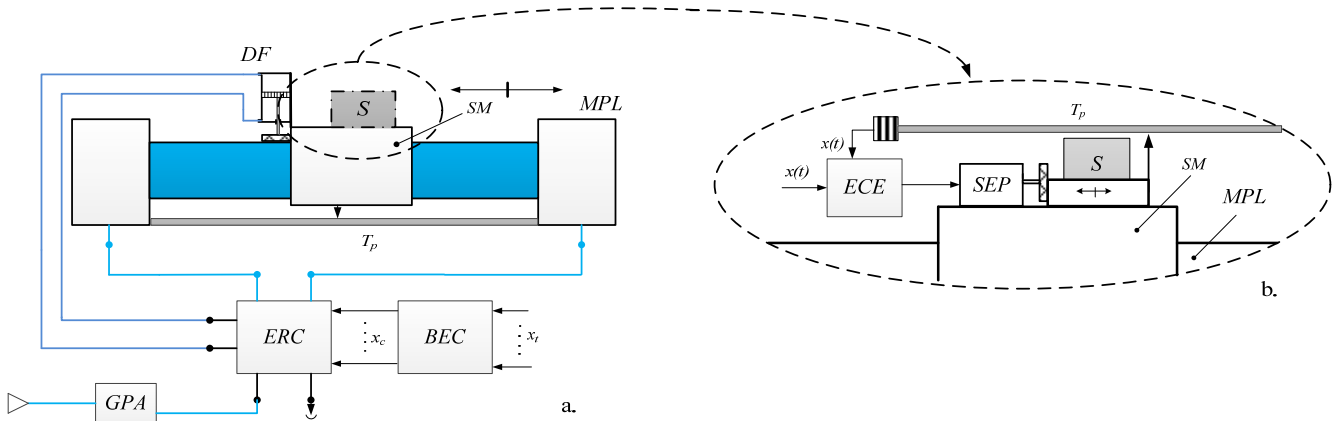


Fig. 1. Principle set-up of an electro-pneumatic positioning system.

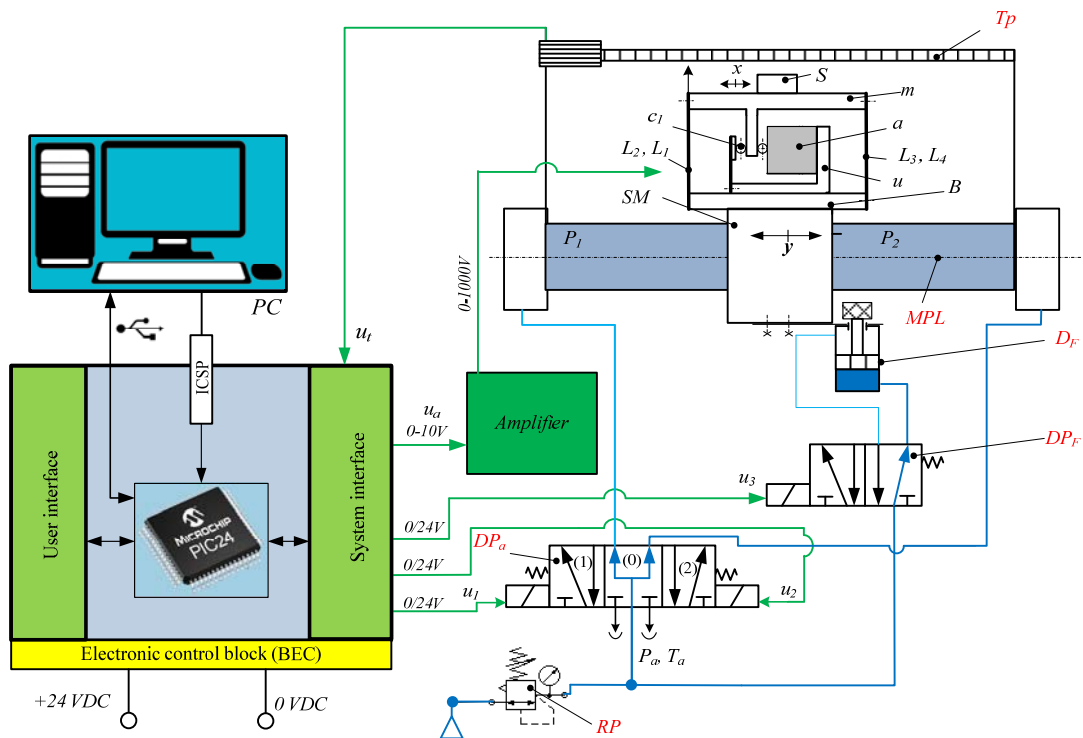


Fig. 2. Detailed set-up of the proposed system.

As it is shown in Fig. 2, the detailed set-up of the proposed system consists of the following subsystems:

- the pneumatic subsystem, consisting of:
  - a pneumatic linear motor *MPL*;
  - a position transducer *T<sub>p</sub>*;
  - a braking device *D<sub>F</sub>*;
  - a pneumatic directional valve *DP<sub>a</sub>* which controls the pneumatic linear motor;
- the compensating piezoelectric subsystem, consisting of:
  - a subassembly mounted on the pneumatically driven slide: the base plate *B*, the special machined part *u* and piezoelectric actuator *a*, which has a levered amplified displacement;



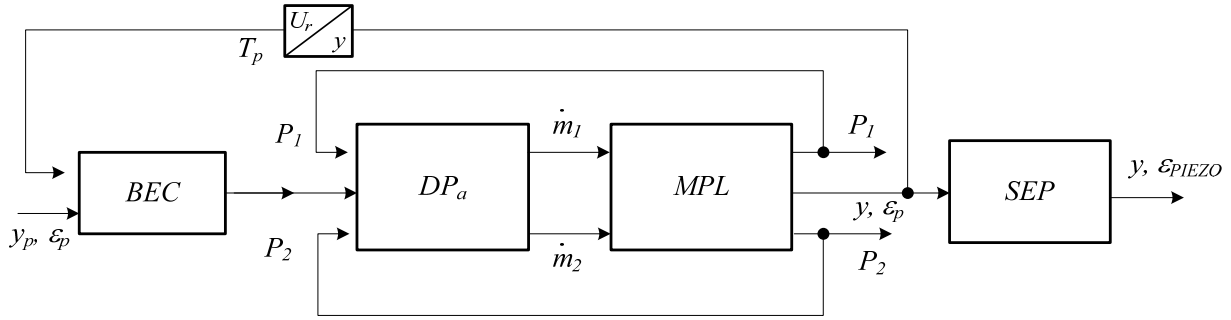


Fig. 5. Modular structure of the system.

Table 2. Notations.

Used notation	Significance
$c$	Maximum travel of the moving stage
$d_n$	Nominal diameter
$D_s$	Diameter of the throttle slide valve
$F_r$	External resistant force
$K$	Constant factor
$\dot{m}_1, \dot{m}_2$	Mass flow rates in the chambers of the pneumatic motor
$m_r$	Mass of the mobile assembly piston – moving stage - load
$P_a$	Supply pressure
$P_1, P_2$	Pressures in the chambers of the motor
$P_0$	Atmospheric pressure
$R$	Universal gas constant
$S$	Active section of the piston
$S_c$	Flow section through the throttle
$T_a$	Absolute temperature
$V_1, V_2$	Volumes of the motor chambers,
$y$	Displacement of the pneumatic moving stage
$x$	Displacement of the throttle slide valve
$x_n$	Nominal opening of the throttle
$\alpha_1$	Shape factor
$\chi$	Adiabatic factor

- the magnetic circuit simplified equation:

$$N \cdot i = \frac{\phi}{\mu_0 \cdot A} \cdot (l_c + d - z) \quad (2)$$

where:  $l_c$  – magnetic core length;  $d$  – initial value of the air gap;  $\mu_r$  – relative magnetic permeability of the core.

- the electric circuit equation:

$$N \cdot (1 + \alpha) \cdot \frac{d\phi}{dt} + R \cdot i = u \quad (3)$$

where:  $\alpha$  is a coefficient used to take into account the eddy current losses within the core;

- the equations of the flowing sections through the directional valve, taking into account the structure of the directional valve being used (Fig. 6):

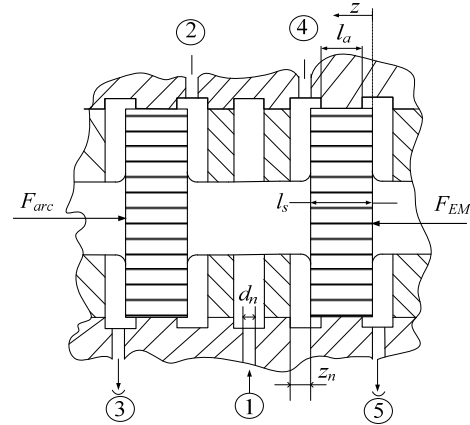


Fig. 6. Section through the way valve.

$$S_{1 \rightarrow 2} = \pi \cdot \frac{d_n^2}{4} \quad (4)$$

$$S_{1 \rightarrow 4} = \begin{cases} \pi \cdot d_s \cdot (z_n - z) & \text{if } 0 \leq t < t_n \\ 0 & \text{if } t_n \leq t < t_{sim} \end{cases} \quad (5)$$

$$S_{4 \rightarrow 5} = \begin{cases} 0 & \text{if } 0 \leq t < t^* \\ \pi \cdot d_s \cdot \left(z - \frac{l_s + l_a}{2}\right) & \text{if } t^* < t \end{cases} \quad (6)$$

where:

$$t^* = \sqrt{\frac{l_s + l_a}{2 \cdot z_{max}}} \cdot t_c \quad (7)$$

$$t_n = \sqrt{\frac{z_n}{z_{max}}} \cdot t_c \quad (8)$$

$$z_n = \frac{d_n^2}{4 \cdot d_s} \quad (9)$$

$t_a$  – switching time, experimentally determined for the directional valve being used;

$z_{max}$  – sliding valve maximum stroke;

The flow rates equation are given by:

$$\dot{m}_1 = \text{sign}(P_a - P_1) \cdot \frac{K \cdot S_{1 \rightarrow 2}}{\sqrt{T_a}} \cdot \max\{P_a, P_1\} \cdot N \left[ \min \left\{ \frac{P_1}{P_a}, \frac{P_a}{P_1} \right\} \right] \quad (10)$$

$$\dot{m}_2 = \begin{cases} \text{sign}(P_2 - P_a) \cdot \frac{K \cdot S_{1 \rightarrow 4}}{\sqrt{T_a}} \cdot \max\{P_2, P_a\} \cdot N \left[ \min \left\{ \frac{P_a}{P_2}, \frac{P_2}{P_a} \right\} \right] & \text{if } 0 \leq t \leq t_n \\ \text{sign}(P_r - P_0) \cdot \frac{K \cdot S_{4 \rightarrow 5}}{\sqrt{T_a}} \cdot \max\{P_r, P_0\} \cdot N \left[ \min \left\{ \frac{P_0}{P_r}, \frac{P_r}{P_0} \right\} \right] & \text{if } t \geq t_n \end{cases} \quad (11)$$

where:  $K = 0,04042 [\sqrt{Ks}/m]$

$$N(x) = \begin{cases} 1 & \text{if } 0 \leq z \leq 0.528 \\ 2,6143 \cdot \sqrt{x^{\frac{2}{\lambda}} - x^{\frac{\lambda+1}{\lambda}}} & \text{if } 0.528 < z \leq 1 \end{cases} \quad (12)$$

In the above equations, it was assumed the same air temperature -  $T_a$  - along the whole flowing path.

- For the pneumatic linear motor, MPL, the functioning equations are:
- the pressure variation within the working chamber  $C_1$ :

$$\frac{dP_1}{dt} = \frac{\chi}{V_{P0} + y \cdot S_p} \cdot \left( \dot{m}_1 \cdot R \cdot T_a - S_p \cdot P_1 \cdot \frac{dy}{dt} \right) \quad (13)$$

- the pressure variation within the working chamber  $C_2$ :

$$\frac{dP_2}{dt} = \frac{\chi}{V_{P0} + (c - y) \cdot S_p} \cdot \left( -\dot{m}_2 \cdot R \cdot T_a - S_p \cdot P_2 \cdot \frac{dy}{dt} \right) \quad (14)$$

- the mobile subassembly piston-moving stage-load movement equation:

$$m_r \cdot \frac{dv}{dt} = (P_1 - P_2) \cdot S_p - c_\eta \cdot v - F \quad (15)$$

After the pneumatic system performed the gross positioning and stopped, the correction stage follows, when the piezoelectric system begins to move the load in order to lower the error. The actuator used for this system is a piezoelectric stack one, with mechanical amplification, type P287 from Physik Instrumente. Its maximum linear displacement is  $700\mu m$  for a supply voltage of  $1000 V$ .

The equivalent scheme of the system is shown in Fig. 7. The following equations can be written:

$$F_a = \beta \cdot y - \gamma \cdot u \quad (16)$$

$$y = \frac{1}{\gamma} \cdot \left[ \int i \cdot dt - (C_s - \beta) \cdot u \right] \quad (17)$$

$$m \frac{d^2y}{dt^2} + c \frac{dy}{dt} + ky = F_a \quad (18)$$

where:

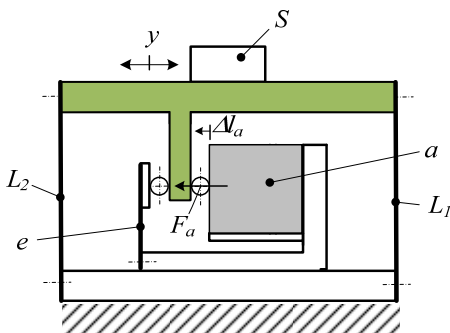


Fig. 7. Set-up of the piezoelectric compensator.

$F_a$  – the output force of the piezoelectric actuator;

$$\beta_{u=0} = \frac{F_a}{\Delta l_a} = 0,13 N/\mu m ;$$

$\gamma = d \cdot N \cdot \frac{k_s}{\lambda}$  and it can be determined by measuring the displacement  $\Delta l_a$ , for a given  $U$ , when  $F_a = 0$ ;

$k_s = \frac{Y \cdot A}{N \cdot h}$  is the stiffness of the entire stack;

$d$  – piezoelectric constant,  $N$  – number of patches,  $Y$  – Young’s modulus,  $A$  – cross section area,  $\lambda$  – displacement amplification of the piezoelectric actuator,  $h$  – thickness of a patch,  $i$  – current through piezoelectric stack;  $s$  – Laplace complex variable;  $C_s$  – stack capacity (catalogue value);  $m$  – mass of the fine positioning moving part;  $c$  – equivalent structural damping coefficient of the elastic guide and return spring;  $k$  – equivalent stiffness of the elastic guide and return spring.

The overall mathematical model is strongly nonlinear and its numerical simulation served mainly for checking over the system capability to perform the desired task, in terms of movement dynamics. Anyway, the experimental research allows for some simplifications in order to ease the integration of the system of equations. The first one is related to the directional valve functioning equations. It is usual to assume a certain time law for the sliding valve displacement,  $z = z(t)$ . Starting from (1) where  $F_0 = F_{fe} - F_{0,arc} - F_a$  is considered to be constant, the movement equation of the mobile subassembly (the mobile armature of the electromagnet and the sliding spool of the directional valve) can be approximately integrated.

Firstly, the real magnetization curve  $B = B(H)$  is linearized as presented in Fig. 8. There are two different zones on this approximate characteristic: a proportional increase of the magnetic flux density,  $B$ , for which the magnetic flux is given by  $\phi = BA \in [0, \phi_s]$ , and a saturation area for which the magnetic flux is constant,  $\phi = B_s \cdot A = \phi_s$ . It is recommended to avoid saturation, but it happens sometimes, when the electromagnet has small dimensions.

Further the first case is considered. After a step voltage is applied to the electromagnet electric circuit ( $t=0$ ), two situations appear (Fig. 9):

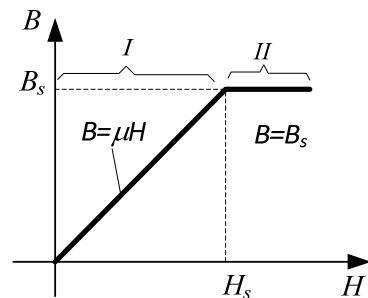


Fig. 8. Approximate magnetization curve.

- for  $t \in [0, t_1]$  the mobile assembly is not moving,  $z=0$ , because the magnetic flux did not reach the value  $\phi_0 = \sqrt{2\mu_0 A F_0}$ , so the force developed by the electromagnet is lower than  $F_0$ ;

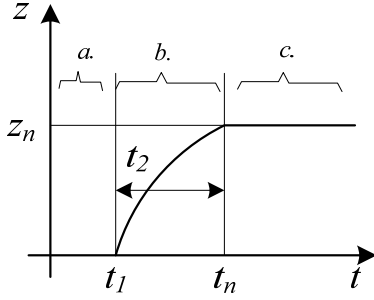


Fig. 9. Step voltage response.

- b. for  $t \in [t_1, t_n]$  the mobile assembly is moving in the range  $[0, z_n]$ , because the value of the magnetic flux is higher than  $\phi_0$ , so the force developed by the electromagnet is higher than  $F_0$ ;

By replacing the current  $i$  given by (2) into (3), it results:

$$\frac{d\phi}{dt} + q\phi - r\phi x - pu = 0 \quad (19)$$

where:

$$q = \frac{R}{\mu_0 AN^2(1+\gamma)} \left( \frac{l_c}{\mu_r} + d \right) \quad (20)$$

$$p = \frac{1}{N(1+\gamma)} \quad (21)$$

$$r = \frac{R}{\mu_0 AN^2(1+\gamma)} \quad (22)$$

For  $t \in [0, t_1]$  the displacement is  $z = 0$  and (19) is simplified, with the solution given by:

$$\phi = \frac{p \cdot u}{q} (1 - e^{-qt}) \quad (23)$$

In this case, the current through the electromagnet coil is:

$$i = \frac{p_1}{q} (1 - e^{-qt}) \quad (24)$$

where:

$$p_1 = p \frac{1}{\mu_0 AN} \left( \frac{l_c}{\mu_r} + d \right) \quad (25)$$

For  $t = t_1$  the magnetic flux is  $\phi = \phi_0$ . In this case, from (23) it results:

$$t_1 = \frac{1}{q} \ln \frac{p \cdot u}{p - q \phi_0} \quad (26)$$

For  $t \in [t_1, t_n]$ , in order to study the dynamics of the mobile assembly (19) and (1) are used. The latter is transformed as:

$$\frac{d^2 z}{dt^2} + \omega^2 \cdot z - n \cdot \phi^2 + f_0 = 0 \quad (27)$$

where:

$$\omega = \sqrt{\frac{k}{m_r}}; \quad n = \frac{1}{2 \cdot \mu_0 \cdot A \cdot m_r}; \quad f_0 = \frac{F_0}{m_r}.$$

For the unknowns related by equations (19) and (27), power series solutions are looked for:

$$z = \alpha_3 t^3 + \alpha_4 t^4 + \alpha_5 t^5 + \dots \quad (28)$$

$$\phi = \phi_0 + \beta_1 t + \beta_2 t^2 + \beta_3 t^3 + \dots$$

By introducing these functions and their derivatives into (19) and (27), it will result two power series with null coefficients and, respectively the coefficients of (28):

$$\beta_1 = p \cdot u - q \cdot \phi_0 \quad (29)$$

$$\beta_2 = -\frac{q}{2} \cdot (p \cdot u - q \cdot \phi_0)$$

$$\alpha_3 = \frac{1}{3} \cdot \phi_0 \cdot (p \cdot u - q \cdot \phi_0)$$

This way, by limiting the number of terms in (28), the valve spool displacement and magnetic flux can be expressed as:

$$z = \alpha_3 \cdot t^3 \quad (30)$$

$$\phi = \phi_0 + \beta_1 t + \beta_2 t^2$$

The lack of access to electromagnet construction data, because the directional valve is a commercial one, coefficients  $\beta_1$ ,  $\beta_2$  and  $\alpha_3$  had to be experimentally determined. For this purpose, the stand presented in fig. 10 was designed and built. It consists of the following devices:

- data acquisition board *DAQ* NI-6009 connected to the PC;
- tested pneumatic directional valve, *DP<sub>a</sub>*;
- calibrated low resistance resistor, *R<sub>1</sub>*;
- pneumatic motor, *MPL*;
- flow transducer, *T<sub>m</sub>*;
- high power driver *ULN2803A*.

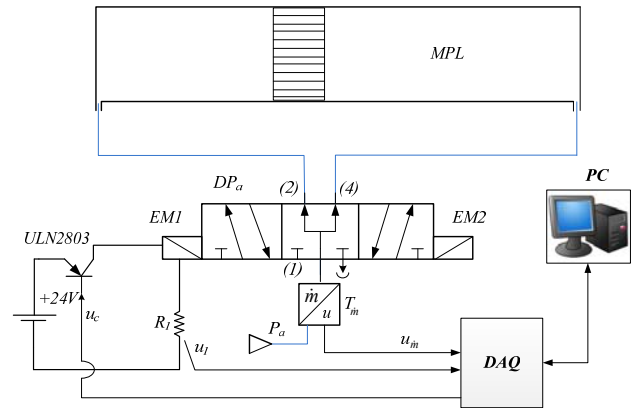


Fig. 10. Test stand schematic.

Fig. 11 shows the three curves determined with this experimental stand:  $u_c(t)$  – input voltage for electromagnet energizing;  $u_l(t)$  – voltage drop on the calibrated resistor, which follows the time variation of the coil current;  $u_m(t)$  – output of the flow transducer, which gives information about the air flow into the left chamber of the pneumatic motor, as well as about the displacement of the electromagnet mobile armature, connected to the valve spool.

These curves are useful for determining:

- $p$ ,  $q$  and  $q'$ ; by choosing two convenient points on the curve  $u_l(t)$  in the interval  $[0, t_1]$  and making use of the equation (24), where  $i = u_1(t)/R_1$  and  $q$  is replaced with  $q' = q(1 + R_1/R)$ , a linear system is

obtained with the unknowns  $p_l$  and  $e^{-q't}$ ;

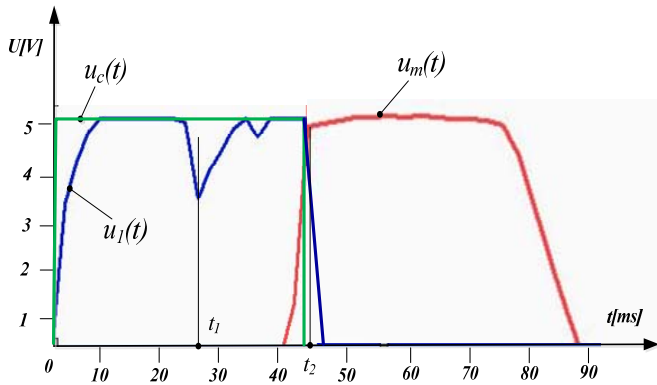


Fig. 11. The characteristic of the electromagnet.

- $p$  from equation (26), after determination of  $t_1$ ;
- $\alpha_3$  from (30), by measuring  $t_2$  without additional resistor,  $R_l$  and knowing the sliding spool displacement,  $z_n$ .

The mathematical model of the dynamic behaviour of the positioning system, described by the equations (4)-(18) was implemented in SIMULINK (Fig. 12). Pneumatic subsystem block and piezoelectric one are presented in Fig.13 and 14, respectively.

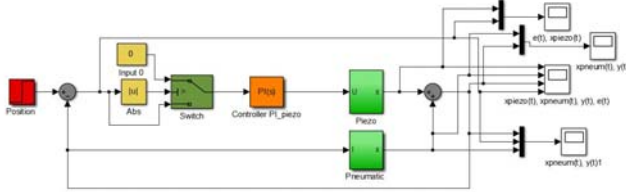


Fig. 12. Simulink application.

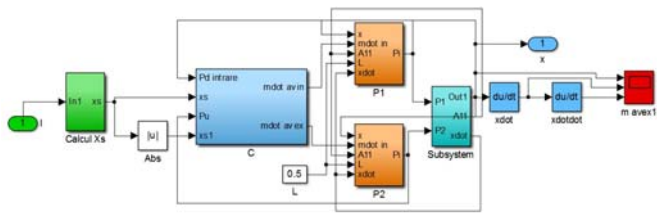


Fig.13. Pneumatic subsystem block.

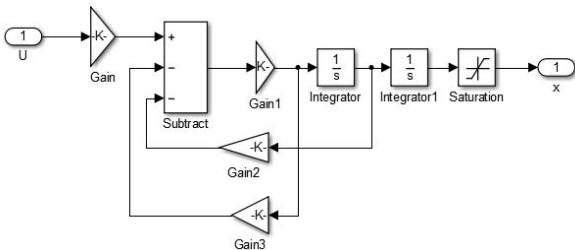


Fig.14. Piezoelectric subsystem block.

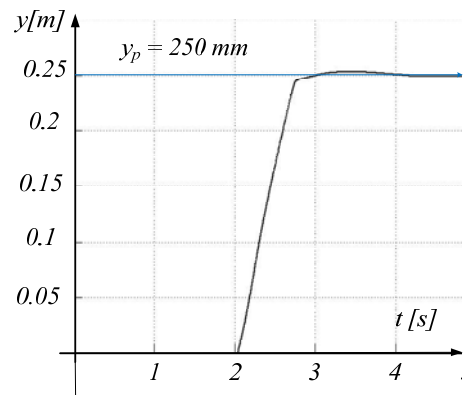
Before running the simulation for the input data  $y_p = 250\text{mm}$ ,  $\epsilon_p = 0,25\text{ mm}$  and  $\epsilon_{\text{piezo}} = 0,1\text{ mm}$ , the position for the beginning of the AL phase should be determined. This

is possible by integration of the equation (15), when the pressure in both motor chambers become equal. This leads to:

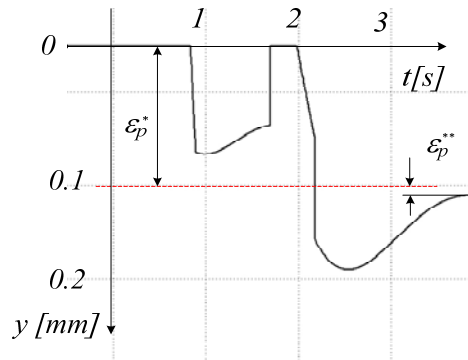
$$y_f = y_p + \frac{m_r v_f^2}{F} - \frac{m_r v_f}{c_\eta} - \frac{F m_r}{c_\eta^2} \ln \frac{F}{c_\eta v_f} \quad (31)$$

where  $v_f$  is the piston velocity at the end of AR phase.

As mentioned above, the simulation has shown the system capability to behave as desired, so the diagram in Fig.12 does not contain the iterative learning controller. Moreover, a switch block can commute from pneumatic model to the piezoelectric one. The simulation of the pneumatic system was run several times with improved initial parameters, derived from the previous results ( $l_f$ ,  $v_f$ ). This way, the pneumatic positioning had rapidly reached the error  $\epsilon_p^* = 0,2\text{ mm}$ , and after introducing the piezoelectric correction the overall error was  $\epsilon_p^{**} = 0,02\text{ mm}$  (Fig.15).



a)



b)

Fig. 15. Simulation results: a) pneumatic positioning; b) piezoelectric positioning.

The simulation results are better than expected, because the model does not take into account some disturbances like the temperature variation, or friction forces, both Coulomb and viscous type. Obtaining a better dynamics during simulation than the real one is not usual. Anyway, its goal was reached as a design stage of the mixed positioning system – pneumatic and piezoelectric, with improved accuracy and low cost control based on microcontroller and directional valves.

4. THE EXPERIMENTAL WORK AND RESULTS

The experimental stand was built according to the principle set-up in Fig. 2. Some components, like pneumatic actuator (MPL), classic directional valves (DP<sub>w</sub>, DP<sub>F</sub>), pneumatic brake (D<sub>F</sub>), position transducer (T<sub>p</sub>), piezoelectric actuator (a - PI 287) or high voltage supply (Amplifier - PI E 472) were commercial ones, while for the piezoelectric correction of the final position, a compliantly guided positioning stage with leaf springs was specially developed.

The electronic control block (BEC) was also developed by the authors. It is based on a PIC24 microcontroller, which runs a program written using C++ and the CCS PIC compiler. This one provides controls to the directional valves amplifiers and to the piezoelectric high voltage supply, according to the iterative learning control (ILC) algorithm for pneumatic positioning and PI for piezoelectric one. The control signals are amplified both for directional valves (ULN 2803A) and for piezoelectric actuator (PI E472).

This program allows the load positioning in any point of the stroke with a certain error. For example, when the positioning is made with pneumatic means, the ILC algorithm search for a more accurate positioning by correcting the braking start position (beginning of the AL stage, in Fig.3) with the simple relationship:

$$y_{f,k+1} = y_{f,k} - \lambda \cdot \varepsilon_{p,k} \tag{32}$$

where:  $\varepsilon_{p,k} = y_p - y_k$  is the positioning error at step  $k$ ;  $y_p$  – desired (target) position;  $y_k$  – the actual position at the end of step  $k$ ;  $\lambda$  – convergence acceleration factor, which should be chosen as  $\lambda > 1$ , if the sign of  $\varepsilon_{p,k}$  remains the same, or  $\lambda < 1$ , if the sign of  $\varepsilon_{p,k}$  alternates.

As an example of experimental results for pneumatic positioning, Fig. 17 shows the steps for refining the load position, in the case of the following values:

- target position,  $y_p = 250 \text{ mm}$ ;
- retracting position,  $y_r = 200 \text{ mm}$ ;
- initial braking position,  $y_f = 220 \text{ mm}$ ;
- assumed pneumatic error,  $\varepsilon_p = 1 \text{ mm}$ .

For the three performed tests, it was obtained a maximum pneumatic gross positioning error,  $\varepsilon_p^* = 0.2 \text{ mm}$ . This is in the working range of the piezoelectric fine positioning stage, which can move the load with smaller steps, as it is shown in Fig.18. This one was experimentally raised and put into correspondence the control voltage applied to the high voltage supply PI E570 and the displacement of the piezoelectric stage.

There are two different curves for voltage increase and decrease, which cause a hysteric behaviour of the piezoelectric stack, but the PI controller and the feedback provided by position transducer (with a 0.025 mm resolution), have led to a final overall positioning error,  $\varepsilon_p^{**} = 0.05 \text{ mm}$ .

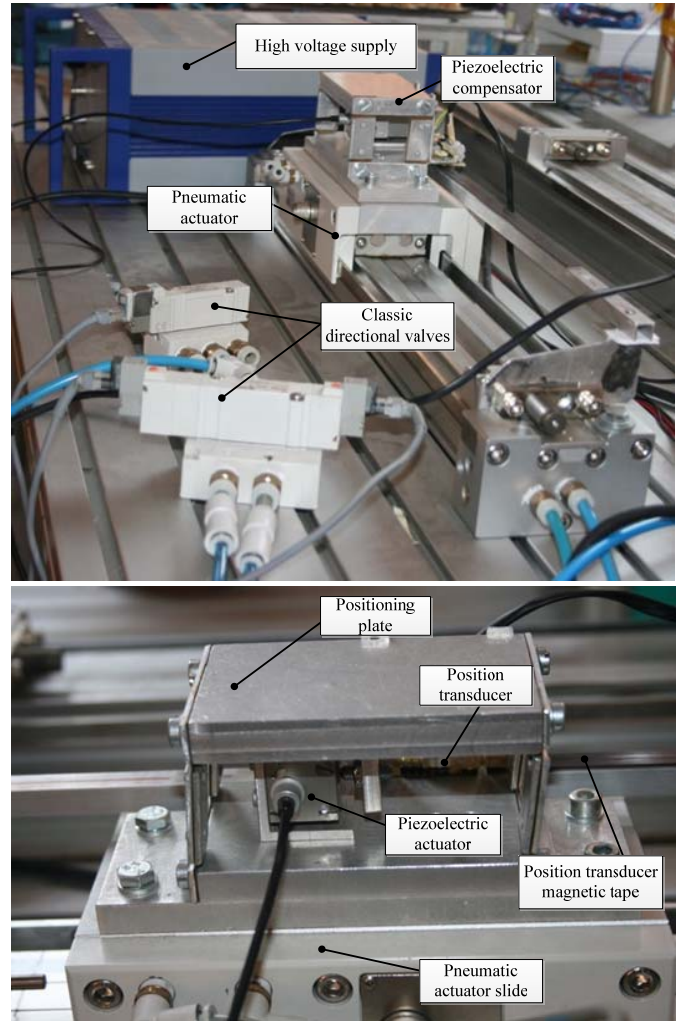


Fig. 16. Views of the experimental model.

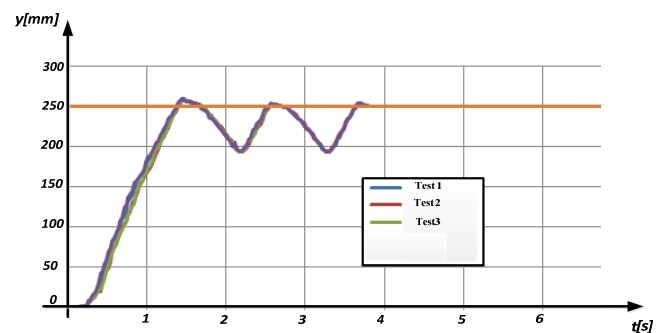


Fig. 17. Experimental results.

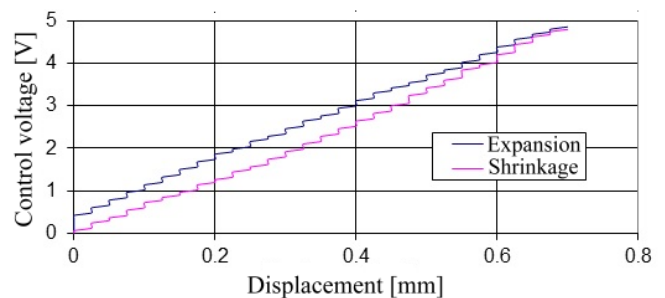


Fig.18. Piezoelectric stage characteristics.

:

## 5. CONCLUSIONS

Pneumatic actuation for positioning is largely used in industrial applications, due to its advantages regarding low costs of the components, low size and mass, high driving forces, ease of velocity control and, very important, safe operation in dangerous environments, with explosion risk.

But air compressibility and temperature variation were an important impediment for obtaining an accurate positioning with classical on-off control, which has led to development of the costly proportional control devices.

The paper proposes a correction method, which allows an important increase of the positioning accuracy of the pneumatic systems. While using classical directional valves, an iterative learning control algorithm can bring the positioning error of the pneumatic actuator in the working range of a piezoelectric actuator. For both actuating systems, which have additional displacements, the feedback from a high resolution position sensor completes the control procedure. The proposed positioning system was tested both by simulation, in order to make the adequate configuration of the system components and during laboratory experiments, which confirmed the assumed performance.

Even the use of the piezoelectric compensating device means a higher complexity of the system, in the end, the cost of the entire system is lower, because the proportional devices are no more needed. Moreover, the positioning accuracy provided by proportional devices control cannot compete with the one of the piezoelectric devices.

The developed hardware structure can be used for implementing different control algorithms in order to improve the performances of the system. This needs further developments.

## REFERENCES

- Avram, M., Duminičă, D., Bucșan, C., Constantin, V. (2011). Hardware and Software Structure of a Pneumo-Hydraulic Positioning System. *Journal of Control Engineering and Applied Informatics*, 13, 2, pp. 20 - 25.
- Bone, G., and Chen, X. (2012). Position Control of Hybrid Pneumatic-Electric Actuators. *2012 American Control Conference Fairmont Queen Elizabeth*, Montréal, Canada June 27-June 29.
- Brian, T., Maul, G., and Jayawiyanto, E. (2005). A Novel, Low-Cost Pneumatic Positioning System. *Journal of Manufacturing Systems*, 24.4, pp. 377-387.
- Chen, X. (2012). Development of a Hybrid Pneumatic-Electric Actuator. *Open Access Dissertations and Theses*. Paper 6822.
- Dihovicni, D., and Novak, N. (2008). Simulation, Animation And Program Support For A High Performance Pneumatic Force Actuator System. *Mathematical and Computer Modelling* 48.5-6, pp. 761-768.
- Hazem, A., and Bashi, S.M. (2009). A Review of Pneumatic Actuators (Modelling and Control). *Australian Journal of Basic and Applied Sciences* 1.1.
- Hodgson, S., Le, M.Q. Tavakoli, M., and Pham, M.T. (2011). Sliding-Mode Control of Nonlinear Discrete-Input Pneumatic Actuators, *IEEE/RSJ International Conference on Intelligent Robots and Systems*, pp. 738-743
- Kolsi-Gdoura, E., Moez, F., and Nabli, D. (2015). Control of a Hydraulic Servo System using Sliding Mode with an Integral and Realizable Reference Compensation. *Journal of Control Engineering and Applied Informatics* 17.1, pp. 111-119.
- Naoki, I., Wakui, S. and Nakamura, Y. (2014). Implementation of Model Following Control for a Pneumatic Stage: Improvement of Repeatability and Positioning Speed. *International Conference on Advanced Mechatronic Systems*.
- Ning, S., and Bone, G.M. (2005). Development of a Nonlinear Dynamic Model for a Servo Pneumatic Positioning System. *IEEE International Conference Mechatronics and Automation*.
- Richer, E., and Yildirim, H. (2000). A High Performance Pneumatic Force Actuator System: Part I—Nonlinear Mathematical Model. *Journal of Dynamic Systems* 122.3, pp. 416.
- Richiedei, D., (2012). Synchronous Motion Control of Dual-Cylinder Electrohydraulic Actuators Through a Non-Time Based Scheme. *Journal of Control Engineering and Applied Informatics* 14, 4, pp.80-89.
- Shih, M., and Ming-An, M. (1998). Position Control of a Pneumatic Cylinder using Fuzzy PWM Control Method. *Mechatronics* 8.3, pp. 241-253.
- Topcu, E., and Yuksel, I. (2006). Development of electro-pneumatic fast switching valve and investigation of its characteristics. *Mechatronics* 16, pp. 365–378.
- Yao, B., Zhou, Z., Liu, Q., and Ai, Q. (2016). Empirical Modeling and Position Control of Single Pneumatic Artificial Muscle. *Journal of Control Engineering and Applied Informatics*, 18, 2, pp. 86-94.
- Yung-Tien, L., and Jiang, C. (2007). Pneumatic Actuating Device with Nanopositioning Ability utilizing PZT Impact Force Coupled with Differential Pressure. *Precision Engineering* 31.3, pp. 293-303.
- Wang, H., Mo, J.P.T., Chen, N. (1996). Hybrid Fuzzy Logic Algorithm for Positioning Control of Pneumatic Actuator with 3/2 Way Solenoid Valves. *Proceedings of the Institution of Mechanical Engineers, Part C: Journal of mechanical engineering science*.